

## Excess fructose enhances the cytotoxicity of unsaturated fatty acid via reactive oxygen species production in hepatocytes

Takehiro YONEZAWA, Keisuke KAKISAKA,  
Yuji SUZUKI, Jo KANAZAWA and Yasuhiro TAKIKAWA

Division of Hepatology, Department of Internal Medicine,  
School of Medicine, Iwate Medical University, Yahaba, Japan

*(Received on January 16, 2020 & Accepted on February 13, 2020)*

### Abstract

The prevalence of metabolic syndromes has increased dramatically in both Western and Asian countries, and nonalcoholic fatty liver disease (NAFLD) has recently emerged as a major health issue. Excess fructose intake is a progressive factor in the pathophysiology of NAFLD. In this study, we aimed to analyze the effects of fructose on hepatocytes during lipotoxicity. The effects of fructose were assessed in mice fed a high-fat diet with/without sucrose (HFDS/HFD) and in HepG2 cells. Mice fed HFDS showed advanced liver fibrosis as compared with mice fed HFD or normal chow. Hemoxygenase-1 expression was significantly increased in the livers of HFDS-fed mice. In MTT assays, oleate induced

cell death in HepG2 cells treated with fructose-supplemented Dulbecco's modified Eagle's medium (DMEM). Although oleate did not cleave Caspase 3, oleate increased necrotic cell death in HepG2 cells cultured in fructose-supplemented DMEM. Oleate in fructose-supplemented DMEM significantly increased the number of reactive oxygen species (ROS)-positive hepatocytes. N-acetyl cysteine ameliorated oleate-induced ROS production and cell death. Although unsaturated fatty acids are less lipotoxic fatty acids, excess fructose can promote unsaturated fatty acid toxicity via ROS production.

**Key words :** *nonalcoholic steatohepatitis, necrosis, oleate, reactive oxygen species, unsaturated free fatty acid*

### I. Introduction

The prevalence of metabolic syndrome has increased among developed countries<sup>1,2)</sup>. Thus, the incidence of nonalcoholic fatty liver disease (NAFLD), a liver phenotype of metabolic syndrome, has also increased<sup>3,4)</sup>. After successful eradication of hepatitis C

virus infection by direct acting antivirals<sup>5)</sup>, nonalcoholic steatohepatitis (NASH), an aggressive form of NAFLD, has become one of the most common causes of liver cirrhosis<sup>6, 7)</sup>. Thus, NAFLD is recognized as not only a health issue but also an economic burden because of a lack of established treatment strategies and therapeutic agents.

Further studies of the pathophysiology of NAFLD are needed to prevent progression to

Corresponding author: Keisuke Kakisaka  
keikaki@iwate-med.ac.jp

NASH. Although the pathogenic mechanism of NASH is thought to be multifactorial, lipid accumulation in hepatocytes is a fundamental characteristic of the disease<sup>8)</sup>. After accumulation of lipids, several insults to hepatocytes, such as exposure to agents associated with intracellular toxicity, activation of innate immunity, or imbalance of the microbiota, may lead to hepatocyte death or liver inflammation<sup>9-12)</sup>. Therefore, lipotoxicity in hepatocytes has been extensively studied<sup>9)</sup>. Saturated free fatty acids (FFAs), such as palmitate (PA), are strong inducers of cytotoxicity via stimulation of apoptotic pathways in hepatocytes<sup>13)</sup>. During these processes, PA induced endoplasmic reticulum stress, c-Jun N-terminal kinase (JNK) phosphorylation, and mitochondrial membrane permeabilization<sup>14)</sup>. In contrast, unsaturated FFAs, such as oleate (OA), are not considered cell death inducers in hepatocytes<sup>15)</sup>. Furthermore, unsaturated FFAs decrease the cytotoxicity of saturated FFAs<sup>15)</sup>. Thus, unsaturated FFAs are thought to be harmless lipids.

Excess intake of fructose can also worsen NASH pathophysiology<sup>16)</sup>. Fructose is a monosaccharide found in fruits, honeys, and vegetables<sup>17)</sup>. High-fructose corn syrup (HFSC) is widely used as a food ingredient, particularly in soft drinks, owing to its sweetness<sup>17)</sup>. Extensive use of HFSC has been reported to be associated with the increased incidence of metabolic syndrome worldwide<sup>16-18)</sup>. In the field of basic research, fructose is a source of FFAs and can induce cell damage via production of reactive oxygen species (ROS)<sup>19, 20)</sup>. In a rodent model of NASH, sucrose supplementation composed of both glucose and fructose induces lobular inflammation

in the liver of the mice with a methionine-choline deficient diet. In this condition, fructose is more cytotoxic than glucose when these two sugars are used as the source of carbohydrate<sup>21, 22)</sup>. However, the toxicity of fructose in hepatocytes with lipids remains unclear.

Accordingly, in this study, we aimed to elucidate the effects of fructose on lipotoxicity in a mouse NASH model and in cultured hepatocytes.

## II. Materials and Methods

### 1. Animals

Male 4-week-old C57BL/6J mice were obtained from Charles River Laboratories (Charles River, Yokohama, Japan) and were housed in humidity-controlled rooms with a 12-h light/12-h dark cycle at 22° C with ad libitum access to drinking water. After 1 week of habituation, three mice were fed normal chow (Cont), four mice were fed a high-fat diet (HFD; HFD-60; Oriental Yeast Co., Tokyo, Japan), and four mice were fed an HFD with sucrose supplementation (42 g/L; HFDS). Each group were fed their respective diet for 16 weeks. All animal experiments were approved by the Animal Care and Use Committee of Iwate Medical University (Morioka, Japan; approval no. 28-001). Serum alanine aminotransferase (ALT), aspartate aminotransferase (AST), and total cholesterol (TC) were measured with an autoanalyzer (cat. no. JCA-BM2250; JEOL, Tokyo, Japan). Animal experiments were approved by an Institutional Animal Care and Use Committee.

### 2. Histological evaluation

Paraformaldehyde-fixed, paraffin-embedded (4%) liver tissue blocks were cut into 3-

$\mu\text{m}$ -thick sections and stained with hematoxylin-eosin staining for steatosis, Masson-Goldner staining for fibrosis, and immunostain for hemocytogenase-1 (HO-1).

### 3. Cells

Huh-7 and HepG2 cells were used as cultured hepatocytes. These cell lines were maintained using 10% fetal bovine serum in Dulbecco's modified Eagle's medium with low glucose (1 g/L). PA and OA were used with the above DMEM with either glucose (3.5 g/L; high glucose) or fructose (3.2 g/L; high fructose) supplementation. These two media contained the same amount of calories per unit volume. Stock concentrations of OA and PA were 160 mM. Cells were treated with 400 or 800  $\mu\text{M}$  of the indicated lipids for confirmation of lipid toxicity.

### 4. Cell proliferation assay

We evaluated cell proliferation using 2-(2-methoxy-4-nitrophenyl)-3-(4-nitrophenyl)-5-(2,4-disulfophenyl)-2H-tetrazolium monosodium salt (WST-8) assays (Nacalai Tesque, Kyoto, Japan), and absorbance was determined using a microplate reader (Multiskan FC; Thermo Fisher Scientific, Yokohama, Japan). Assays were performed according to instructions of the kit manufacturer. Briefly, cells were seeded into 96-well plates 24 h before the examination. After removed of the medium from each well, 100  $\mu\text{L}$  medium with the indicated FFAs or solvent as a control was added, and cells were incubated for 16 h. SF agent (10  $\mu\text{L}$ ) was added to each well, and the absorbance at 450 nm was measured 0 and 2 h later. Background absorbance at 450 nm was subtracted. The ratio of that relative to the control group was reported to determine cell proliferation.

### 5. Cell death assay

To evaluate cell death, cells were stained using an Apoptotic/Necrotic/Healthy Cells Detection Kit (PromoCell GmbH, Heidelberg, Germany), according to the manufacturer's instructions. Briefly, cells on cover glass in 6-well plates were treated with different media for various times. Fluorescein isothiocyanate-annexin V, ethidium homodimer III, and Hoechst 33342 were mixed with binding buffer, and the mixture was added to the cells. After incubation for 15 min, cells were visualized using fluorescent microscopy. Red staining indicated necrotic cells, whereas green staining indicated apoptotic cells. Results were expressed as the ratio of the number of dyed cells to the number of nuclei (stained blue). Assays were performed at least three times.

### 6. Detection of ROS

Cells on cover glass in 6-well plates were treated with different media for various times. To evaluate ROS production, CellROX Green Reagent (cat. no. 10422; Thermo Fisher Scientific, Waltham, MA, USA) was added to each well at a concentration of 5  $\mu\text{M}$ . Cells were incubated for 30 min at 37°C. After fixation with 3.7% formaldehyde for 15 min, cells on the cover glass were mounted in a mounting medium with 4', 6-diamidino-2-phenylindole. Cells were visualized using fluorescent microscopy. Green punctate dots indicated ROS. Results were expressed as the ratio of the number of cells with punctate dots to the number of nuclei. ROS production was determined in at least four images of high-power fields.

### 7. Immunohistochemistry of HO-1 positive cells in the liver

Anti HO-1 antibody was used for staining

Table 1. PCR primers in this study

Gene	Forward or Reverse primer	Primer sequence (5' -3')
<i>α</i> SMA	Forward	ctctctccagccatcttcat
<i>α</i> SMA	Reverse	tataggtggttcgtggatgc
Collagen I	Forward	ccgctgggtcaagatggtc
Collagen I	Reverse	ctccagcctttccaggttct
Collagen III	Forward	ctcctgggtgagcgaggac
Collagen III	Reverse	gaccaggttgcccatcact
GAPDH	Forward	gggttcctataaatcggactgc
GAPDH	Reverse	ccattttgctacgggacga

on paraffin-embedded liver sections of the mice. After incubation with primary antibody, the sections were incubated with peroxidase-labeled anti-mouse secondary antibodies (Histofine Simple Stain Max-PO Kit, Nichirei, Tokyo, Japan). Then, 3,3'-diaminobenzine was used for signal development in the presence of peroxidase. Results were expressed as the ratio of the number of cells with HO-1 positive staining to the number of nuclei.

### 8. Immunoblotting analysis

Whole-cell lysates were prepared as described previously. Equal amounts of protein (20–40  $\mu$ g) were resolved by sodium dodecyl sulfate-polyacrylamide gel electrophoresis on 4–12% acrylamide gels and transferred to polyvinylidene difluoride membranes. The membranes were incubated with primary antibodies at 4°C overnight and were then incubated with the appropriate horseradish peroxidase-conjugated secondary antibodies at room temperature for 90 min (BioSource International, Camarillo, CA, USA). Bound antibodies were visualized using a chemiluminescent substrate (ECL Prime, Amersham, Buckinghamshire, UK).

### 9. Quantitative reverse transcription polymerase chain reaction (qRT-PCR)

Total cellular RNA was extracted using

TRIzol reagent (Invitrogen, Camarillo, CA, USA) and was reverse transcribed into cDNA with Moloney murine leukemia virus reverse transcriptase (Invitrogen) and random primers (Invitrogen). cDNA was used as a template for qRT-PCR, which was carried out on a LightCycler instrument (Roche Applied Science) using SYBR green (Molecular Probes, Eugene, OR) as a fluorophore. PCR primers are summarized in Table 1. Gene expression was quantified by the  $2^{-\Delta\Delta Ct}$  method, and the target mRNA expression levels were expressed relative to glyceraldehyde 3-phosphate dehydrogenase in each sample.

### 10. Reagents and antibodies

For immunoblotting analysis and immunohistochemistry, the following primary antibodies were used: goat anti- $\beta$ -actin (1:1000; cat. no. sc-1616; Santa Cruz Biotechnology, Santa Cruz, CA, USA), anti-hemoxygenase-1 (HO-1; 1:30 for immunohistochemistry; cat. no. sc-136960; Santa Cruz Biotechnology), anti-phosphorylated c-Jun (1:1000; cat. no. 9261; Cell Signaling Technology, Tokyo, Japan), anti-phosphorylated JNK (1:1000; cat. no. 9251; Cell Signaling Technology), and anti-cleaved caspase 3 (1:1000; cat. no. 9661; Cell Signaling Technology). N-acetyl cysteine (NAC) was purchased from Sigma (St. Louis, MO, USA).

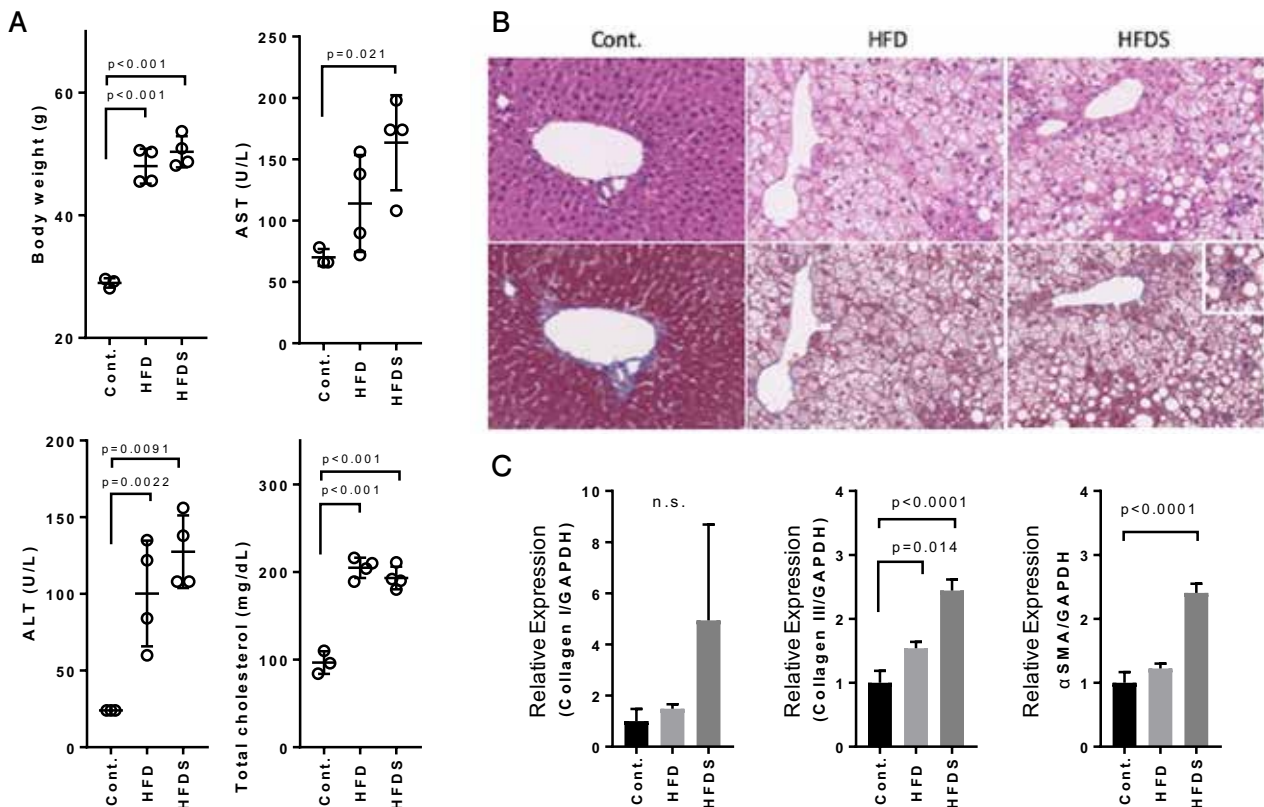


Fig. 1. Effects of a high-fat diet (HFD) with or without sucrose on weight gain, liver enzymes, hypercholesteremia, liver inflammation, and liver fibrosis.

A: Body weight (upper left panel), aspartate aminotransferase (upper right panel), alanine aminotransferase (lower left panel), and total cholesterol (lower right panel) after 16 weeks of feeding were evaluated in mice fed normal chow (Cont), an HFD, or an HFD with sucrose (HFDS).

B: Representative microscopic images of liver sections subjected to hematoxylin and eosin staining (upper panels, magnification,  $50\times$ ) and Masson's trichrome staining (lower panels, magnification,  $50\times$ ) for histological evaluation. Left, middle, and right panels are the Cont, HFD, and HFDS groups, respectively.

C: mRNA expression of the indicated genes as analyzed by qRT-PCR. Data are the means  $\pm$  SDs.

NAC was dissolved in phosphate-buffered saline to obtain a 2 M stock solution.

## 11. Statistical analysis

All data represent the results of at least three independent experiments and are expressed as the mean  $\pm$  standard deviation. The differences between the groups were compared using Student's t-test and one-way analysis of variance with a *post-hoc* Dunnett's test. All statistical analyses were performed using the SPSS 17.0 software program (SPSS Inc., Chicago, IL, USA). Results were considered significant when the p-value was  $<0.05$ .

## III. Results

### 1. HFD induced steatosis in mice, and sucrose supplementation enhanced HFD-induced inflammation and fibrosis in the liver

To confirm the effects of the HFDS, we compared the results for body weight, histological findings of the liver, and laboratory data among the HFDS, HFD and Cont groups. Body weight was significantly higher in the HFD and HFDS groups than in the Cont group (Fig. 1A). AST levels were significantly higher in the HFDS group than in the Cont

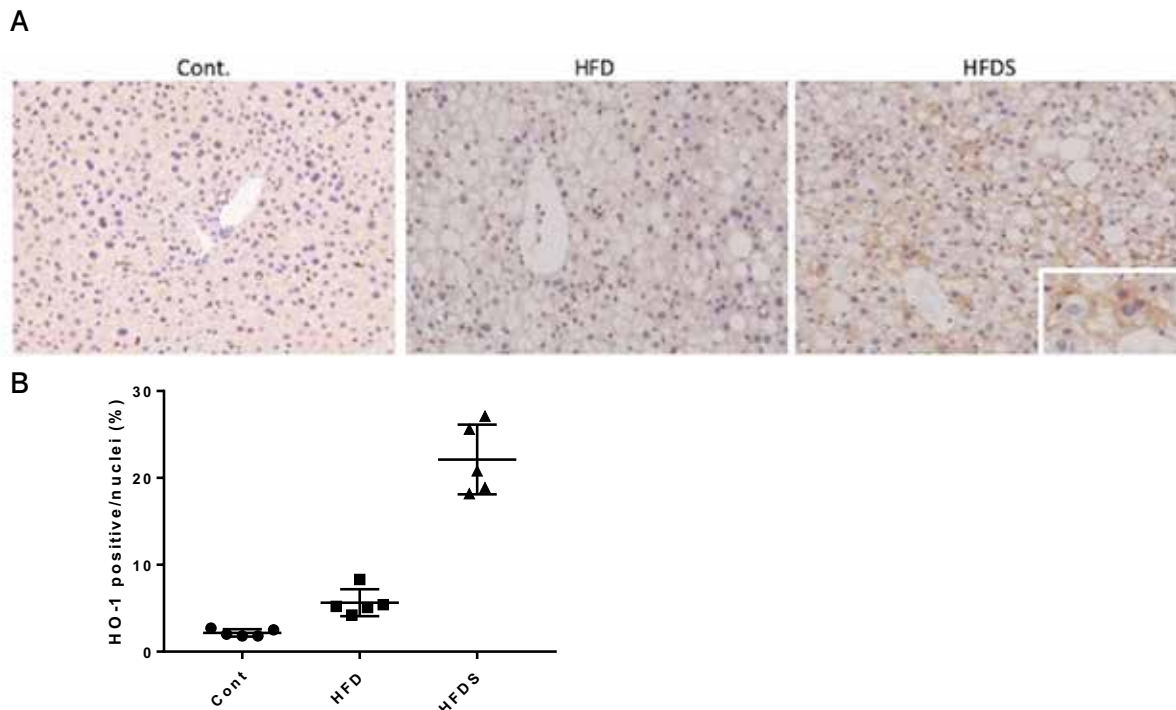


Fig. 2. Mice fed a high-fat diet (HFD) with sucrose (HFDS) showed increased levels of hemoxygenase-1 (HO-1) in the liver.

A: Immunohistochemical analysis of HO-1. Left, middle, and right panels indicate groups fed normal chow (Cont), a high-fat diet (HFD) and high fat diet with sucrose (HFDS), respectively.

B: HO-1 positive hepatocytes were detected by light microscopy. HO-1-positive hepatocytes were counted in at least five images of high-power fields. Data are the means  $\pm$  SDs (\* $p < 0.05$ ).

group (Fig. 1A). ALT and TC levels were significantly higher in the HFD and HFDS groups than in the Cont group (Fig. 1A). In histological analyses, overt lipid accumulation in the liver was found in both the HFD and HFDS groups (Fig. 1B). Furthermore, lymphocyte accumulation was found in the HFDS group. No advanced fibrosis was observed in the HFD and HFDS groups (Fig. 1B). However, mRNA expression of  $\alpha$ -smooth muscle actin and collagen III was significantly higher in livers in the HFDS group than in livers in the Cont group; in contrast, collagen I expression did not differ among these mice (Fig. 1C). These data indicated that HFDS induced steatohepatitis with fibrogenic changes, suggesting that this may be a good model of early-stage NASH.

## 2. HFDS increased HO-1 expression in the liver

Because sucrose is composed of both glucose and fructose, and fructose is known as an inducer of ROS, we hypothesized that fructose was the primary cause of sucrose-induced liver injury in the mice with HFDS. To elucidate whether sucrose supplementation had effects similar to those of fructose on inducing ROS production, we evaluated HO-1 expression in the liver. HO-1 is known as a marker of ROS production because expression of HO-1 responds to chemical and physical agents that directly or indirectly generate ROS. The positive area of HO-1 staining in hepatocytes increased significantly in the HFDS group compared with those in the Cont

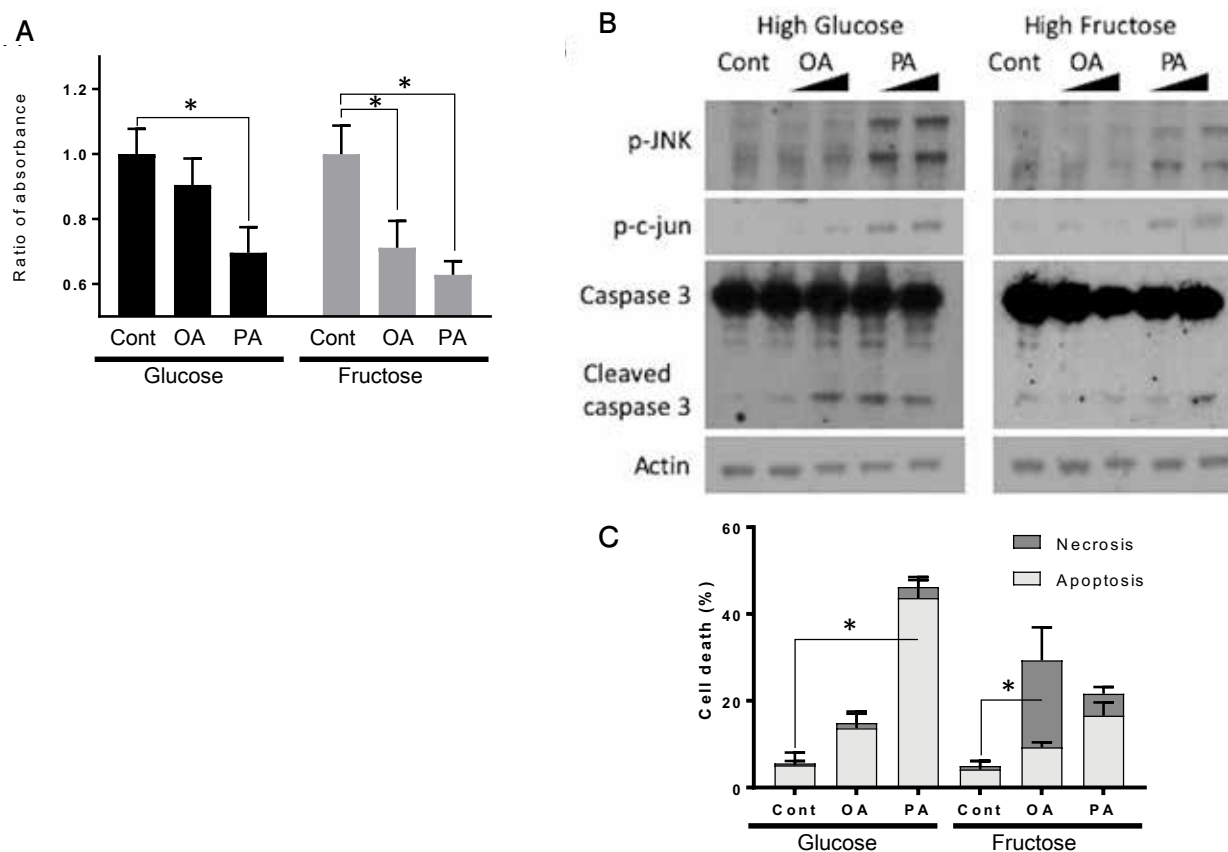


Fig. 3. Fructose supplementation enhanced OA-induced cytotoxicity via necrosis in a caspase-independent manner. A and C: HepG2 cells were incubated with OA (800  $\mu$ M) or PA (800  $\mu$ M) for 16 h. Vehicle-treated cells were used as controls (Cont). Three conditions were evaluated under two types of media: glucose-supplemented (Glucose) or fructose-supplemented medium (Fructose). Cell proliferation was assessed using SF reagents (A). Cell death was assessed using an Apoptotic/Necrotic/Healthy Cells Detection Kit, and apoptosis and necrosis were detected using fluorescent microscopy. Results were expressed as the ratio of the number of dyed cells to the number of nuclei (blue) (C). B: Immunoblot analysis of phosphorylated JNK, phosphorylated c-Jun, caspase 3, and actin. Whole-cell lysates were prepared from HepG2 cells after incubation with OA (800  $\mu$ M), PA (800  $\mu$ M), or control (vehicle) treatment for 6 h. Data are the means  $\pm$  SDs (\* $p$  < 0.05).

and HFD groups (Fig. 2A). The number of HO-1-positive hepatocytes was also increased in the HFDS group (Fig. 2B).

### 3. Fructose-supplemented medium enhanced OA-induced cytotoxicity

Because sucrose supplementation induced steatohepatitis in our current model and excess fructose has been shown to be associated with increase prevalence of NAFLD in human studies, we next evaluated how fructose affects lipotoxicity in hepatocytes

in vitro. To confirm the effects of fructose-supplemented medium on hepatocyte viability, cell proliferation assays were performed. In HepG2 cells treated with 800  $\mu$ M PA, cytotoxicity was observed for both glucose-supplemented and fructose-supplemented media (Fig. 3A). In contrast, OA-induced cytotoxicity was only observed in cells with fructose-supplemented medium. Huh-7 and HepG2 cells exhibited OA-induced cytotoxicity when fructose was added to the medium,

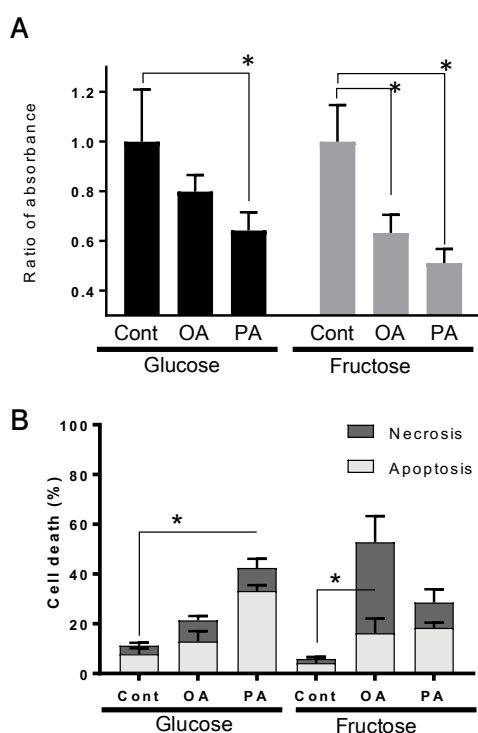


Fig. 4. Fructose supplementation enhanced OA-induced cytotoxicity via necrosis in Huh-7 cells.

A and B: Huh-7 cells were incubated with OA (800  $\mu$ M) or PA (800  $\mu$ M) for 16 h. Vehicle-treated cells were used as controls (Cont). Three conditions were evaluated under two types of media: glucose-supplemented (Glucose) or fructose-supplemented medium (Fructose). Cell proliferation was assessed using SF reagents (A). Cell death was assessed using an Apoptotic/Necrotic/Healthy Cells Detection Kit, and apoptosis and necrosis were detected using fluorescent microscopy. Results were expressed as the ratio of the number of dyed cells to the number of nuclei (blue) (B).

although PA-induced cytotoxicity occurred in both glucose-supplemented and fructose-supplemented media (Fig. 4A).

#### 4. Fructose enhanced OA cytotoxicity in a caspase-independent manner

To determine the mechanisms of OA-induced cytotoxicity, novel signaling pathways associated with lipotoxicity were

evaluated in HepG2 cells using immunoblot analysis. In HepG2 cells treated with 800  $\mu$ M OA in fructose-supplemented medium, phosphorylation of JNK and c-Jun was not observed (Fig. 3B). Furthermore, cleaved caspase 3 did not increase in these cells. In contrast, OA induced cleaved caspase-3 in glucose-supplemented medium. PA induced the phosphorylation of both JNK and c-Jun in both glucose-supplemented and fructose-supplemented media. Cleavage of caspase-3 by PA increased in both glucose-supplemented and fructose-supplemented media, although the effects in glucose-supplemented medium were more dramatic (Fig. 3B).

#### 5. OA-induced cytotoxicity in fructose-supplemented medium was associated with necrosis

To determine the mechanisms through which fructose enhanced OA-induced cytotoxicity, we confirmed the type of cell death using fluorescent microscopy. In HepG2 cells, PA induced apoptosis in both glucose-supplemented and fructose-supplemented media, although the apoptosis rate was higher in glucose-supplemented medium (Fig. 3C). In contrast, necrosis was significantly increased following OA treatment with fructose-supplemented medium. Similar results were observed in Huh-7 cells (Fig. 4B).

#### 6. OA increased ROS production in hepatocytes cultured in fructose-supplemented medium

To confirm the mechanisms through which OA plus fructose induced cell death, evaluated ROS production under each condition. Both glucose-supplemented and fructose-supplemented media without OA did not increase ROS production (Fig.

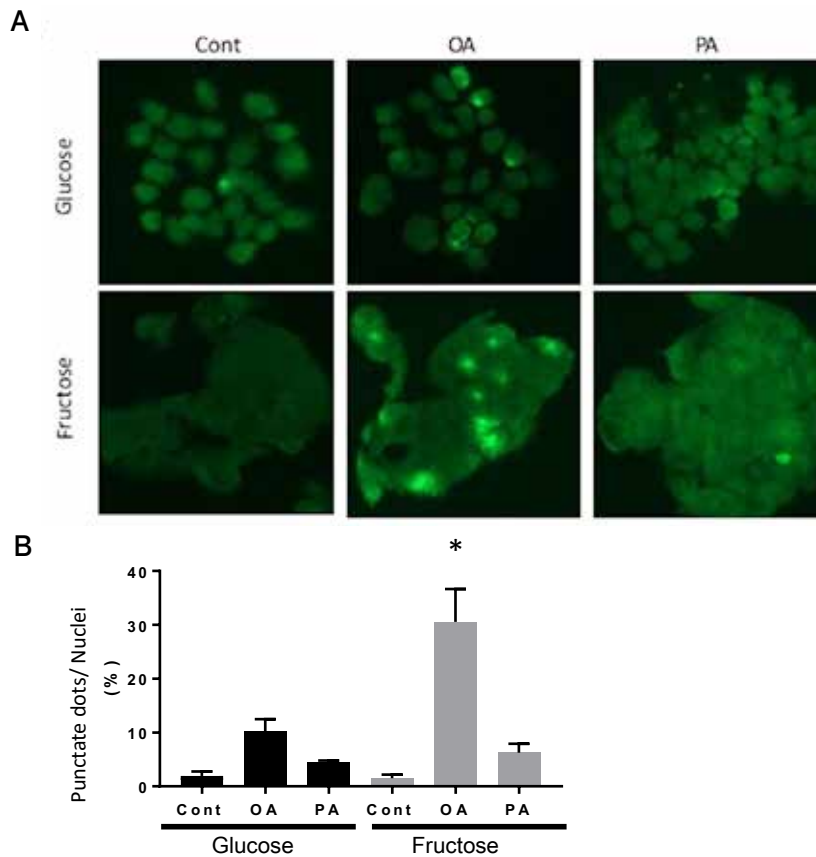


Fig. 5. OA with fructose supplementation induced reactive oxygen species (ROS) production.

A: ROS levels were assessed by CellROX Green Reagent. Images were obtained by fluorescent microscopy. Left, middle, and right panels indicate control (Cont), OA, and PA treatments, respectively. Upper and lower panels indicate glucose-supplemented (Glucose) and fructose-supplemented medium (Fructose), respectively.

B: Punctate dots were counted. Results were expressed as the ratio of the number of cells with punctate dots to the number of nuclei. ROS production was evaluated in at least four images of high-power fields. Data are the means  $\pm$  SDs (\* $p < 0.05$ ).

5A and 5B). In contrast, OA with fructose-supplemented medium increased ROS production, whereas OA with glucose-supplemented medium did not. Although PA induced cell death, PA did not increase ROS production (Fig. 5A and 5B).

### 7. NAC prevented OA-induced ROS production and attenuated OA-induced necrosis in fructose-supplemented medium

We speculated that ROS mediated OA-induced cell death in fructose-supplemented

medium. Thus, we investigated the effects of NAC, a known ROS scavenger, on OA-induced cytotoxicity in fructose-supplemented medium. Our results showed that 2 mM NAC decreased ROS production in combination with OA and fructose-supplemented medium in HepG2 cells (Fig. 6A and 6B) and attenuated OA-induced cytotoxicity (Fig. 6C). In addition, NAC decreased the number of necrotic cells following OA treatment (Fig. 6D).

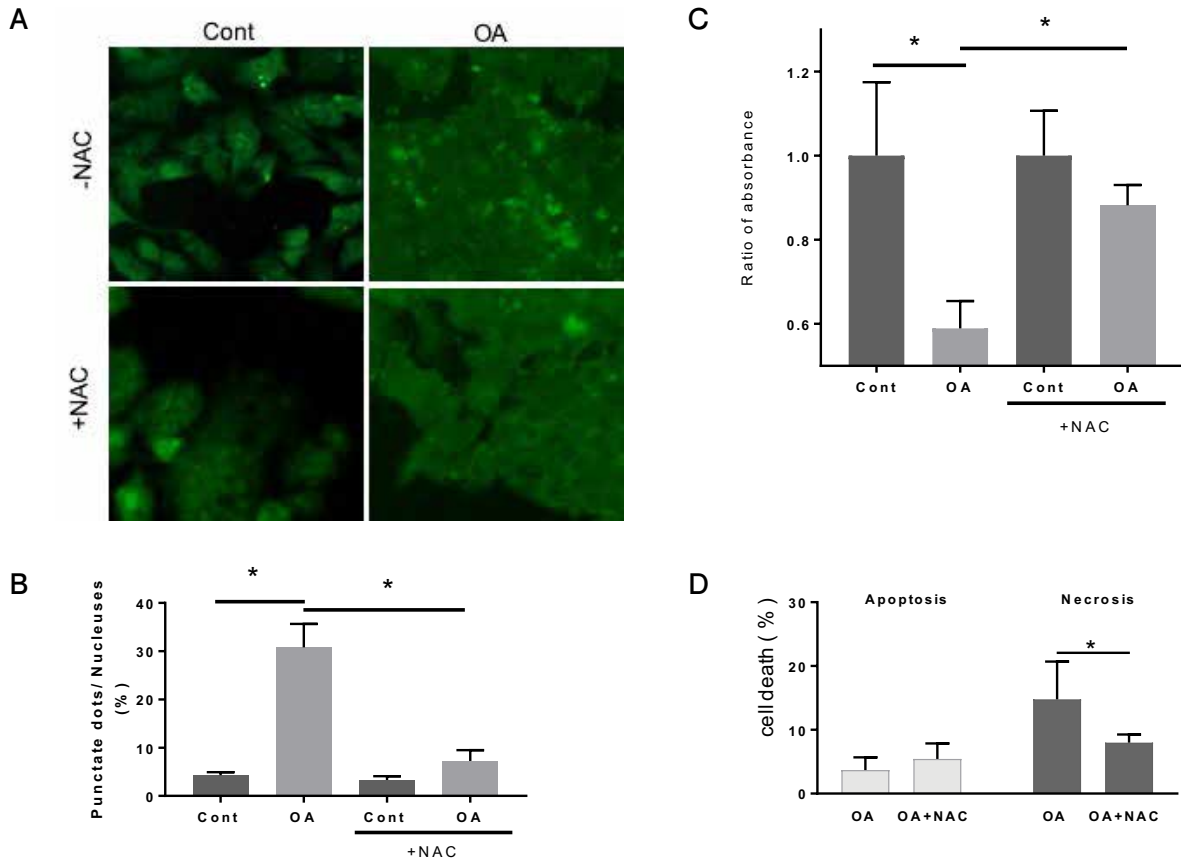


Fig. 6. N-acetyl cysteine (NAC) attenuated OA-induced reactive oxygen species (ROS) production and attenuated OA cytotoxicity by decreasing necrosis.

A: ROS levels were assessed using CellROX Green Reagent. Images were obtained using fluorescent microscopy. Left and right panels indicate control (Cont) and OA treatments, respectively. Upper and lower panels indicate without/with NAC, respectively.

B: Punctate dots were counted. Results were expressed as the ratio of the number of cells with punctate dots to the number of nuclei. ROS production was evaluated in at least four images of high-power fields.

C and D: HepG2 cells were incubated with control (Cont) or OA (800  $\mu$ M) with/without 2 mM NAC in fructose-supplemented medium for 10 h. Vehicle-treated cells were used as controls (Cont). Cell proliferation was assessed using SF reagents (C). Cell death was assessed using an Apoptotic/Necrotic/Healthy Cells Detection Kit, and apoptosis and necrosis were detected using fluorescent microscopy. Results were expressed as the ratio of the number of dyed cells to the number of nuclei (blue) (D). Data are the means  $\pm$  SDs (\* $p$  < 0.05).

#### IV. Discussion

In this study, we demonstrated that HFDS induced steatohepatitis and increased HO-1 expression in the liver. Moreover, we found that OA was cytotoxic in hepatocytes cultured in medium containing high levels of fructose and that OA-induced cytotoxicity in fructose-supplemented medium involved

caspase-independent necrosis mediated by ROS production.

FFAs are causal agents of NASH pathophysiology. In particular, saturated FFAs and their metabolites induce hepatocyte apoptosis via endoplasmic reticulum stress, JNK phosphorylation, and caspase 3 cleavage<sup>14, 23-25</sup>. In contrast, unsaturated FFAs

are believed to be harmless because they do not induce apoptosis and can attenuate the cytotoxic effects of saturated FFAs<sup>15</sup>. However, in this study, we demonstrated that unsaturated FFAs may contribute to liver toxicity under specific conditions, such as in the presence of fructose.

Increased fructose intake is associated with an increased prevalence of obesity in the United States<sup>17</sup>. Therefore, excess fructose intake may be associated with disease progression in NAFLD. In intracellular metabolism, fructose supplies adenosine triphosphate without a suppressive mechanism because there is no rate-limiting enzyme in this pathway<sup>26</sup>. Thus, excess fructose induces mitochondrial function enhancement and depletion of adenosine triphosphate<sup>19,20</sup>. However, the detailed mechanisms of ROS production by unsaturated FFAs plus fructose supplementation remain unclear.

In this study, we found that unsaturated FFAs induced cytotoxicity in the presence of excess fructose. Importantly, fructose itself did not induce significant cytotoxicity and ROS production in this setting, whereas OA induced cell death. These results revealed that the presence of both OA and fructose led to cell death in hepatocytes and demonstrated that unsaturated FFAs may cause insults associated with NASH in the liver. Furthermore, in our *in vivo* NASH model, HO-1, a known marker of the oxidative stress response, was increased in hepatocytes, suggesting that HFDS induced oxidative stress in the liver. Taken together, our findings provide new evidences demonstrating that ROS production was associated with NASH pathophysiology and revealed the mechanisms

through which ROS were generated in NASH. Innate immunity plays a key role in the pathophysiology of NASH because crosstalk between innate immunity and cell death induces liver inflammation, which leads to progression of fibrosis<sup>27</sup>. In NASH, control of hepatocyte death is crucial. As described above, unsaturated FFAs are thought to be harmless lipids that are not associated with the pathophysiology of NASH. However, in this study, we found that OA induced necrosis when cultured with excess fructose. According to previous studies of necrosis, this type of cell death strongly induces inflammation via release of damage-associated molecular patterns<sup>28</sup>. Thus, the necrosis observed in this study may induce significant inflammation *in vivo*. It is still unclear whether apoptosis or necrosis needs to be inhibited during the treatment of NASH. However, *in vivo* inhibition of apoptosis has been reported to promote cancer development<sup>29</sup>. Moreover, undead hepatocytes may yield ballooned hepatocytes, a hallmark of NASH associated with disease severity in the livers of patients with NASH<sup>22, 30</sup>. Furthermore, apoptosis in macrophages ameliorates liver fibrosis<sup>31</sup>. Thus, it is possible that inhibition of apoptosis could have varying effects on the pathogenesis of NASH. Intriguingly, necrostatin, an inhibitor of programmed necrosis (necroptosis), was found to alleviate symptoms of NASH in an *in vivo* model<sup>32,33</sup>. According to the results of this study and previous studies, we speculated that control of necrosis may be a therapeutic target for the treatment of NASH.

There were several limitations to this study. First, oxidative stress was only confirmed by HO-1 expression. Although

we attempted to determine the expression levels of novel oxidative stress markers, such as 8-hydroxydeoxyguanosine, liver samples fixed using paraformaldehyde showed abundant nonspecific staining in the control. Therefore, such markers were inadequate for analysis of oxidative stress. Second, we did not confirm the results using primary hepatocytes. However, we believe that the results of this study would also be observed in primary cells because two cell lines (Huh-7 and HepG2 cells) showed the same results. Third, we did not confirm our results in human NASH. Although we understand the importance of human studies, confirmation is difficult because fructose intake would be challenging to quantify in patients with NAFLD. Thirdly, sucrose instead of fructose was used for *in vivo* study although fructose was used for *in vitro* study. However, a previous study has reported that there are no significant difference of metabolic or endocrine response in health-related effects between HFCS and sucrose<sup>34</sup>). Therefore,

in this study, fructose cytotoxicity in the *in vitro* study may be recapitulated by the effect of sucrose supplementation in the *in vivo* study. Finally, the mechanisms through which the combination of excess fructose and OA produced ROS remain unknown. Accordingly, further studies of ROS production under these conditions are necessary in order to elucidate the mechanisms of NASH pathophysiology.

We conclude that excess fructose can promote unsaturated fatty acid toxicity via ROS production although the detailed mechanism by which fructose generates ROS during lipotoxicity remains unknown.

#### Acknowledgements

This work was supported by a KAKENHI grant (grant no. JP18K07980, to K.K.).

Conflict of interest: The authors have no conflict of interest to declare.

#### References

- 1) **Chooi YC, Ding C and Magkos F:** The epidemiology of obesity. *Metabolism* **92**, 6–10, 2019.
- 2) **Shin D, Kongpakpaisarn K and Bohra C:** Trends in the prevalence of metabolic syndrome and its components in the United States 2007–2014. *Int J Cardiol* **259**, 216–219, 2018.
- 3) **Estes C, Razavi H, Loomba R, et al.:** Modeling the epidemic of nonalcoholic fatty liver disease demonstrates an exponential increase in burden of disease. *Hepatology* **67**, 123–133, 2018.
- 4) **Kanwal F, Kramer JR, Duan Z, et al.:** Trends in the burden of nonalcoholic fatty liver disease in a United States cohort of veterans. *Clin Gastroenterol Hepatol* **14**, 301–308, 2016.
- 5) **Chen Q, Ayer T, Bethea E, et al.:** Changes in hepatitis C burden and treatment trends in Europe during the era of direct-acting antivirals: a modelling study. *BMJ Open* **9**, doi: 10.1136/bmjopen-2018-026726.
- 6) **Byass P:** The global burden of liver disease: a challenge for methods and for public health. *BMC Med* **12**, 159, 2014.
- 7) **Pimpin L, Cortez-Pinto H, Negro F, et al.:** Burden of liver disease in Europe: epidemiology and analysis of risk factors to identify prevention policies. *J Hepatol* **69**, 718–735, 2018.
- 8) **Diehl AM and Day C:** Cause, pathogenesis, and treatment of nonalcoholic steatohepatitis. *N Engl J Med* **377**, 2063–2072, 2017.
- 9) **Akazawa Y and Nakao K:** To die or not to die: death signaling in nonalcoholic fatty liver disease. *J Gastroenterol* **53**, 893–906, 2018.
- 10) **Hirsova P, Ibrahim SH, Gores GJ, et al.:**

- Lipotoxic lethal and sublethal stress signaling in hepatocytes: relevance to NASH pathogenesis. *J Lipid Res* **57**, 1758–1770, 2016.
- 11) **Ibrahim SH, Hirsova P and Gores GJ:** Non-alcoholic steatohepatitis pathogenesis: sublethal hepatocyte injury as a driver of liver inflammation. *Gut* **67**, 963–972, 2018.
  - 12) **Sawada Y, Kawaratani H, Kubo T, et al.:** Combining probiotics and an angiotensin-II type 1 receptor blocker has beneficial effects on hepatic fibrogenesis in a rat model of non-alcoholic steatohepatitis. *Hepatol Res* **49**, 284–295, 2019.
  - 13) **Malhi H, Barreiro FJ, Isomoto H, et al.:** Free fatty acids sensitise hepatocytes to TRAIL mediated cytotoxicity. *Gut* **56**, 1124–1131, 2007.
  - 14) **Cazanave SC, Mott JL, Elmi NA, et al.:** JNK1-dependent PUMA expression contributes to hepatocyte lipoapoptosis. *J Biol Chem* **284**, 26591–26602, 2009.
  - 15) **Akazawa Y, Cazanave S, Mott JL, et al.:** Palmitoleate attenuates palmitate-induced Bim and PUMA up-regulation and hepatocyte lipoapoptosis. *J Hepatol* **52**, 586–593, 2010.
  - 16) **Basciano H, Federico L and Adeli K:** Fructose, insulin resistance, and metabolic dyslipidemia. *Nutr Metab* **2**, 5, 2005.
  - 17) **Dhingra R, Sullivan L, Jacques PF, et al.:** Soft drink consumption and risk of developing cardiometabolic risk factors and the metabolic syndrome in middle-aged adults in the community. *Circulation* **116**, 480–488, 2007.
  - 18) **Nakagawa T, Tuttle KR, Short RA, et al.:** Hypothesis: fructose-induced hyperuricemia as a causal mechanism for the epidemic of the metabolic syndrome. *Nat Clin Pract Nephrol* **1**, 80–86, 2005.
  - 19) **Gaspers LD, Thomas AP, Douard V, et al.:** Mechanisms underlying fructose-induced oxidative stress in the cytosol and mitochondria. *Biophys J* **98**, 377a, 2010.
  - 20) **Jaiswal N, Maurya CK, Pandey J, et al.:** Fructose-induced ROS generation impairs glucose utilization in L6 skeletal muscle cells. *Free Radic Res* **49**, 1055–1068, 2015.
  - 21) **Pickens MK, Ogata H, Soon RK, et al.:** Dietary fructose exacerbates hepatocellular injury when incorporated into a methionine-choline-deficient diet. *Liver Int* **30**, 1229–1239, 2010.
  - 22) **Pickens MK, Yan JS, Ng RK, et al.:** Dietary sucrose is essential to the development of liver injury in the methionine-choline-deficient model of steatohepatitis. *J Lipid Res* **50**, 2072–2082, 2009.
  - 23) **Kakisaka K, Cazanave SC, Fingas CD, et al.:** Mechanisms of lysophosphatidylcholine-induced hepatocyte lipoapoptosis. *Am J Physiol Gastrointest Liver Physiol* **302**, G77–84, 2012.
  - 24) **Kakisaka K, Cazanave SC, Werneburg NW, et al.:** A hedgehog survival pathway in 'undead' lipotoxic hepatocytes. *J Hepatol* **57**, 844–851, 2012.
  - 25) **Bandla H, Dasgupta D, Mauer AS, et al.:** Deletion of endoplasmic reticulum stress-responsive co-chaperone p58 (IPK) protects mice from diet-induced steatohepatitis. *Hepatol Res* **48**, 479–494, 2018.
  - 26) **Hannou SA, Haslam DE, McKeown NM, et al.:** Fructose metabolism and metabolic disease. *J Clin Invest* **128**, 545–555, 2018.
  - 27) **Arrese M, Cabrera D, Kalergis AM, et al.:** Innate immunity and inflammation in NAFLD/NASH. *Dig Dis Sci* **61**, 1294–1303, 2016.
  - 28) **Schaefer L:** Complexity of danger: the diverse nature of damage-associated molecular patterns. *J Biol Chem* **289**, 35237–35245, 2014.
  - 29) **Takehara T, Liu X, Fujimoto J, et al.:** Expression and role of Bcl-xL in human hepatocellular carcinomas. *Hepatology* **34**, 55–61, 2001.
  - 30) **Suzuki A, Kakisaka K, Suzuki Y, et al.:** c-Jun N-terminal kinase-mediated Rubicon expression enhances hepatocyte lipoapoptosis and promotes hepatocyte ballooning. *World J Gastroenterol* **22**, 6509–6519, 2016.
  - 31) **Higashiyama M, Tomita K, Sugihara N, et al.:** Chitinase 3-like 1 deficiency ameliorates liver fibrosis by promoting hepatic macrophage apoptosis. *Hepatol Res*, doi: 10.1111/hepr.13396, 2019.
  - 32) **Afonso MB, Rodrigues PM, Carvalho T, et al.:** Necroptosis is a key pathogenic event in human and experimental murine models of non-alcoholic steatohepatitis. *Clin Sci* **129**, 721–739, 2015.
  - 33) **Roychowdhury S, McCullough RL, Sanz-Garcia C, et al.:** Receptor interacting protein 3 protects mice from high-fat diet-induced liver injury. *Hepatology* **64**, 1518–1533, 2016.
  - 34) **Stanhope KL, Griffen SC, Bair BR, et al.:** Twenty-four-hour endocrine and metabolic profiles following consumption of high-fructose corn syrup-, sucrose-, fructose-, and glucose-sweetened beverages with meals. *Am J Clin Nutr* **87**, 1194–1203, 2008.

フルクトースの過剰摂取が活性酸素産生を介して  
肝細胞に対する不飽和脂肪酸の  
細胞毒性を増強させる

米澤剛広, 柿坂啓介,  
鈴木悠地, 金沢 条, 滝川康裕

岩手医科大学医学部, 内科学講座消化器内科肝臓分野

*(Received on January 16, 2020 & Accepted on February 13, 2020)*

要旨

欧米及びアジア諸国ではメタボリックシンドロームや非アルコール性脂肪性肝疾患 (NAFLD) の罹患率が飛躍的に増加している。果糖の過剰摂取は NAFLD の増悪因子とされるが、脂肪毒性における果糖の影響は不明である。本研究は脂肪毒性における果糖の細胞障害機序を解明することを目的とした。果糖の効果は蔗糖添加及び無添加の高脂肪食 (HFDS/HFD) を与えたマウスと HepG2 細胞 (ヒト肝癌由来細胞株) で評価した。HFDS を与えたマウスは対照群と比較して肝臓の

線維化が進展し、ヘムオキシゲナーゼ-1 発現も有意に増加した。細胞増殖アッセイで不飽和脂肪酸は果糖添加処理した培養液で培養した HepG2 細胞の細胞死を誘発した。細胞死はカスパーゼ 3 の活性化を伴わない経路で誘発され、活性酸素種 (ROS) の発生を増加させた。これらは N-アセチルシステイン添加処理を加えると改善した。不飽和脂肪酸は果糖の過剰摂取により ROS 産生を介して脂肪毒性を促進する可能性がある。